fs-Mat

A.V. Bulgakov[1], *I. Mirza*[1], *V.A. Volodin*[2], *N.M. Bulgakova*[1]

[1] FZU – Institute of Physics AS CR, Prague, Czech Republic

[2] Novosibirsk State University, Novosibirsk, Russia

E-mail: bulgakov@fzu.cz

Non-thermal ultrashort-pulsed laser annealing of semiconductors at the nanoscale: Crystallization without melting

FemtoMat-2025, Mauterndorf, Austria, February 26, 2025

SENDISO

Co-funded by the European Union

MINISTRY OF EDUCATION, YOUTH AND SPORTS

GAČR CZECH SCIENCE FOUNDATION

FZÚ

Motivation

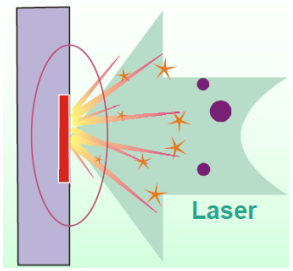

Irradiation of bandgap materials with powerful laser beams

Two opposite research aims:

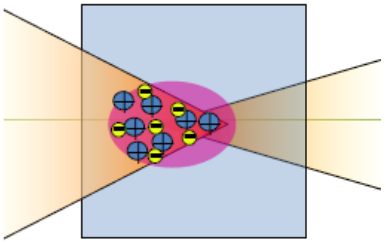

(1) To avoid damage: unwanted modification/cracking/defects in optics

(2) To increase energy coupling into a localized volume for achieving extreme states of matter.

A large field in between: how to gently modify material properties for laser direct writing of photonic structures to enable light manipulations.

Scope of our research

- to learn how laser energy can be coupled in bandgap materials in the most efficient way;
- to predict and control the damage on the desired level, at a smallest volume;
- to reach the highest possible stress level
- to induce phase transitions without material melting

Annealing of nanoscale semiconductor

As-prepared semiconductor nanostructures are usually amorphous and, for most applications, need to be converted into a crystalline form.

Main annealing methods

- Furnace annealing – time- and energy-consuming and unsuitable for low-melt substrates.
- Laser annealing – fast and highly localized but laser-annealed nanostructures are often destroyed by melting.

Here we consider gentle non-thermal melting-free annealing of semiconductor nanostructures with low-fluence ultrashort laser pulses initiating solid-state explosive crystallization.

a-Ge/a-Si multi-nano-layer stack (PECVD)

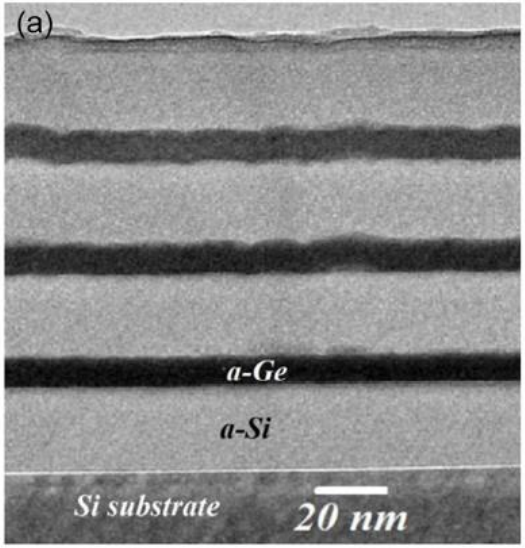

Ge NCs in an amorphous Si matrix are promising for:

- Increasing of quantum efficiency of solar cells
- Improving sensitivity of photodiodes
- Extension of the spectral range of light-emitting diodes
- Optoelectronics

Selective crystallization is needed!

Optical properties of as deposited MNL stack

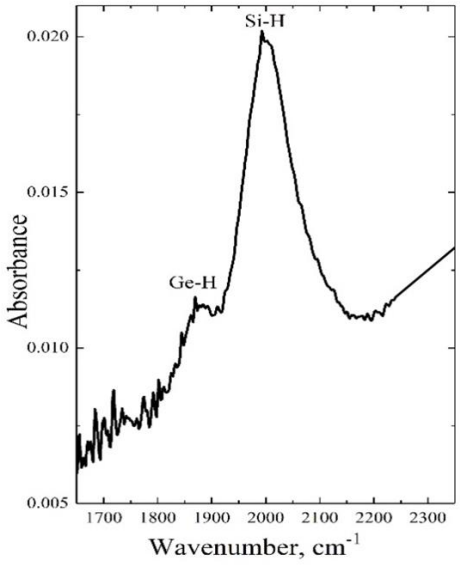

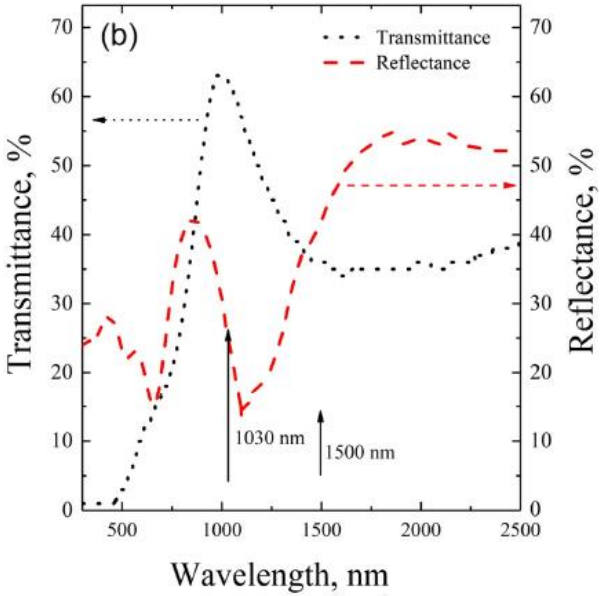

Lasers for annealing:

(1) HiLASE PERLA-B, **1030 nm**, 1.4 ps, up to 10 mJ/pulse

(2) Astrella (Coherent) in combination with an OPA (TOPAS, Light Conversion), **1500 nm**, 70 fs, up to 0.4 mJ.

Laser modification-damage-ablation

Spots at 1500 nm

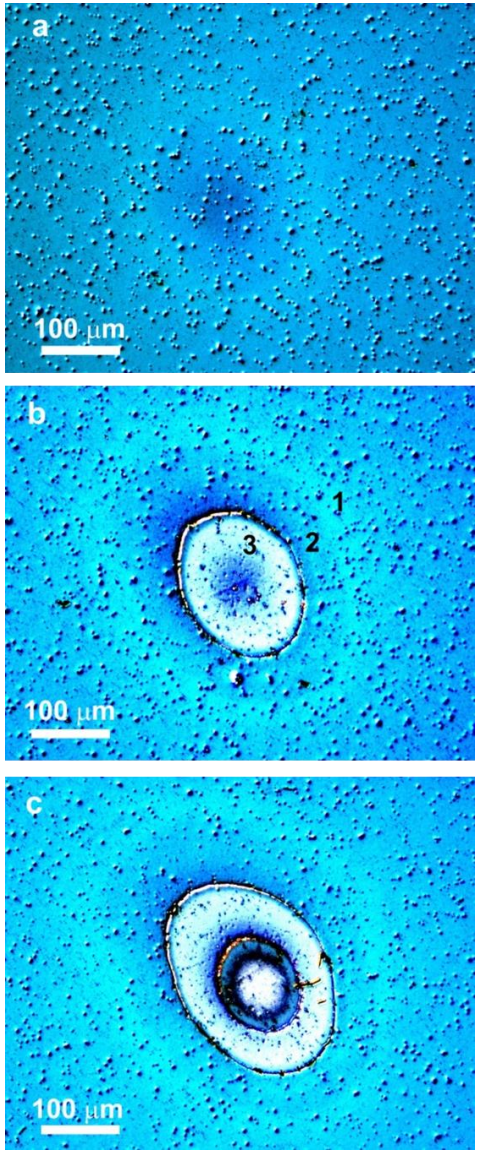

D^2-analysis

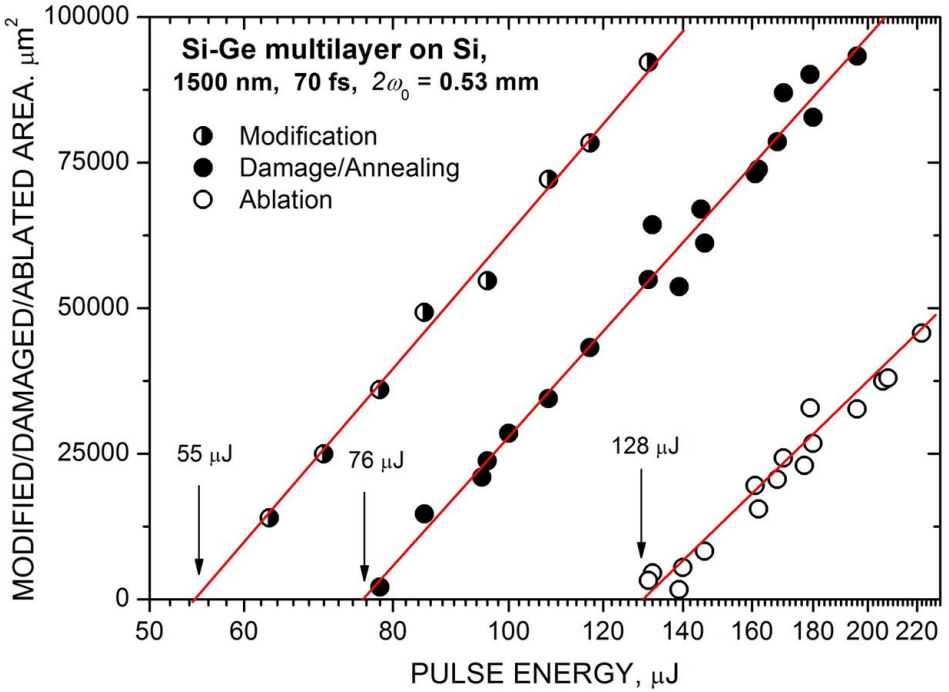

Modification, damage and ablation thresholds

Laser conditions	$F_{th,m}$, mJ/cm²	$F_{th,d}$, mJ/cm²	$F_{th,a}$, mJ/cm²
1500 nm, 70 fs	50	70	115
1030 nm, 1.4 ps	45	65	110

V.A. Volodin, et al., *Opt. Laser Technol.* **161** (2023) 109161

Phase composition of laser-processed Si/Ge MNL stack. Raman spectra

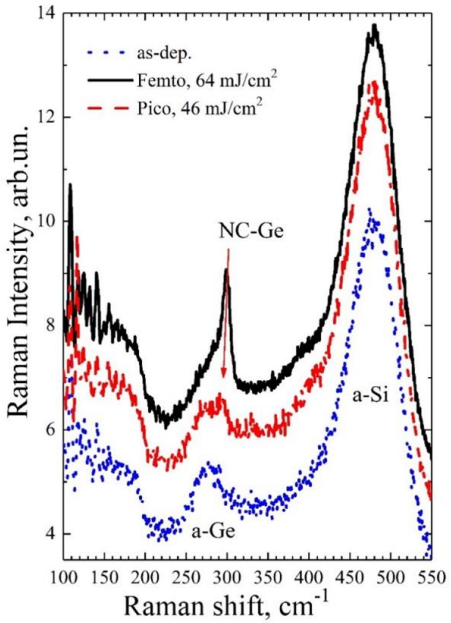

Low fluences below the damage threshold (DT). Arrow shows a peak of Ge NCs.

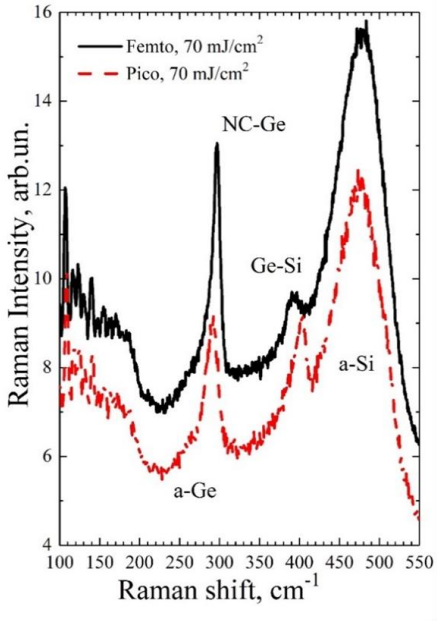

Low-middle fluences near the damage threshold.

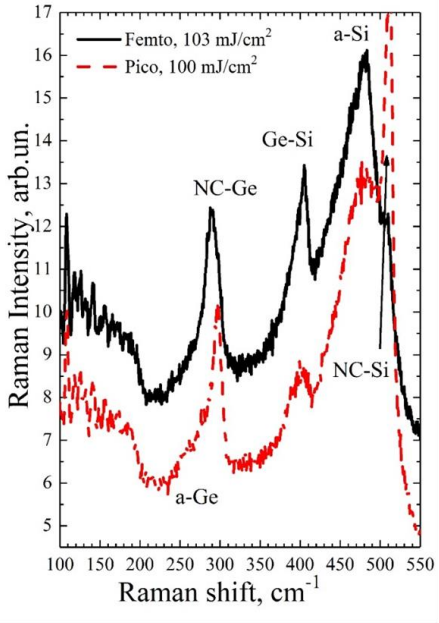

Middle fluences above the DT but below the ablation threshold (AT). The arrow shows a peak of Si NCs.

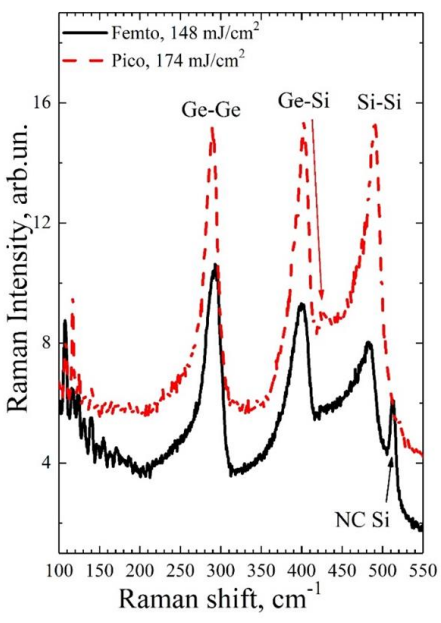

High fluences above the AT. The arrows show a peak of Si NCs (fs pulse) and that of intermixed Si/Ge layers (ps pulse)

Strong peak of Ge NCs is observed with 1500-nm pulses at low fluence, below the DT. No Si crystallization and no intermixing of Si and Ge layers occur under these conditions

V.A. Volodin, et al., *Opt. Laser Technol.* **161** (2023) 109161, A,V. Bulgakov, et al., *Materials* **16** (2023) 3572

Theoretical analysis

Photo-ionization free-electron plasma generation

1PA 2PA collisions Auger

$$\frac{\partial n_e}{\partial t} = \frac{(1-R)\alpha I(z,t)}{\hbar\omega} + \frac{(1-R)^2\beta I^2(z,t)}{2\hbar\omega} + \delta(T_e)n_e - Cn_e^2 n_h.$$

(collisions and Auger terms crossed out)

$$n_e \sim \frac{(1-R)\alpha I\tau}{\hbar\omega} + \frac{(1-R)^2\beta I^2\tau}{2\hbar\omega} = \frac{(1-R)\alpha F}{\hbar\omega} + \frac{(1-R)^2\beta F^2}{2\hbar\omega\tau}$$

Heating of the MNL stack: $c_p\rho\Delta T = (E_g + E_{\mathrm{av}}^e)$

Molten fraction: $f = c_p(T - T_m)/\Delta H_m$

Estimation results

1500 nm, 70 fs

Fluence, mJ/cm²	a-Si			a-Ge				
	n_e, cm^{-3} (1PI)	n_e, cm^{-3} (2PI)	T, K	n_e, cm^{-3} (1PI)	n_e, cm^{-3} (2PI)	$T_0+\Delta T$, K	T - fΔH_m, K	f
55	$2.96\cdot10^{15}$	$6.43\cdot10^{18}$	302	$1.34\cdot10^{21}$	$7.3\cdot10^{20}$	710	710	0
70	$3.77\cdot10^{15}$	$1.04\cdot10^{19}$	303.4	$1.95\cdot10^{21}$	$1.18\cdot10^{21}$	896	896	0
100	$5.39\cdot10^{15}$	$2.12\cdot10^{19}$	306.7	$3.5\cdot10^{21}$	$2.4\cdot10^{21}$	1370	985	0.36
150	$8.09\cdot10^{15}$	$4.78\cdot10^{19}$	315	$7.05\cdot10^{21}$	$5.4\cdot10^{21}$	2457	1396	1

1030 nm, 1.4 ps

Fluence, mJ/cm²	a-Si			a-Ge			
	n_e, cm^{-3} (1PA)	n_e, cm^{-3} (2PA)	T, K	n_e, cm^{-3} (1PA)	$T_0+\Delta T$, K	T - fΔH_m, K	f
55	$6.9\cdot10^{16}$	$4.05\cdot10^{18}$	301	$4.9\cdot10^{21}$	1430	985	0.42
70	$8.75\cdot10^{16}$	$6.56\cdot10^{18}$	302	$6.23\cdot10^{21}$	1737	985	0.709
100	$1.25\cdot10^{17}$	$1.34\cdot10^{19}$	304.2	$8.9\cdot10^{21}$	2353	1292	1
150	$1.88\cdot10^{17}$	$3\cdot10^{19}$	310	$1.34\cdot10^{22}$	3391	2330	1

2PA process dominates in Si. In Ge, at 1500 nm, 1PA and 2PA are comparable.

No melting in Ge for 1500 nm at < 80 mJ/cm². Si remains cold in both cases.

Stresses. Explosive crystallization

Upon annealing, the hot amorphous Ge film located between adjacent cold Si nanolayers experiences thermal tensile stresses. The stress can be evaluated as [1]

$$\sigma_r = \frac{E\alpha_l \Delta T}{2(1-\nu)}$$

Here E is Young's modulus, α_l is the coefficient of linear expansion, ν is the Poisson ratio.

For 1500-nm irradiation, the stresses in the Ge nanolayers can be then estimated as ~ 0.35 GPa for 40 mJ/cm^2 and ~ 1 GPa for 100 mJ/cm^2. The stress can be even higher due to the Ge and Si lattice mismatch.

The stresses of such a level can trigger a process of explosive crystallization [2-3]. The heat released in explosive crystallization provides a propagation of a "crystallization wave", resulting in the efficient a-Ge solid phase crystallization without appearance NC-Si and Ge-Si intermixing.

[1] Y.P. Meshcheryakov, N.M. Bulgakova, *Appl. Phys. A* **82** (2006) 363.
[2] R.K. Sharma, et al. *J. Appl. Phys*. **55** (1984) 387.
[3] C. Césari, et al. *Surf. Sci*. **162** (1985) 724.

Titania nanotubes

TiO_2 = highly functional semiconductive material

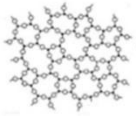
amorphous

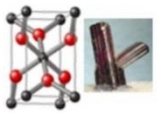
rutile

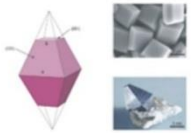
anatase

- High chemical and mechanical stability
- Biocompatiblity
- High conductivity
- High photocatalytic activity
- Cheap

Only anatase combines all these important properties

What are TiO_2 nanotubes films?

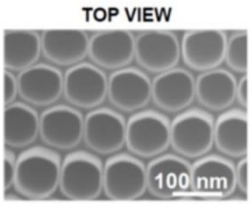

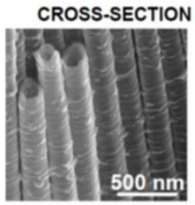

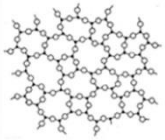
amorphous as grown

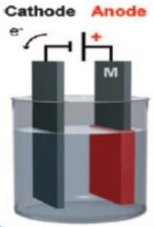

Grown by Electrochemical Anodization of Titanium
Diameter ~100 nm (0.0001 mm)
Length ~ 1-20 µm

Problem: Transformation of amorphous TiO_2 NTs into anatase

Potential applications of TiO_2 NT arrays in anatase form

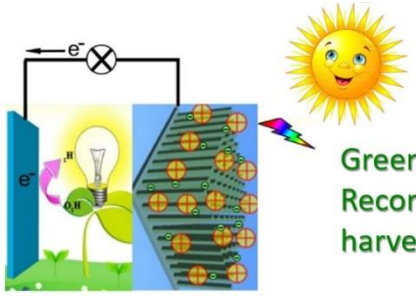

Green energy: Record solar energy harvesting

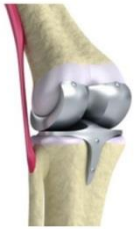

Biocompatible coatings for implants

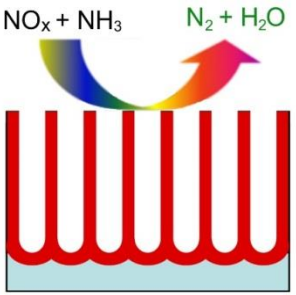

Green chemistry: Efficient catalysing for pollutants reduction

Imani et al. Advances in Biomembranes and Lipid Self-Assembly, 2016, Volume 24, p. 163-207

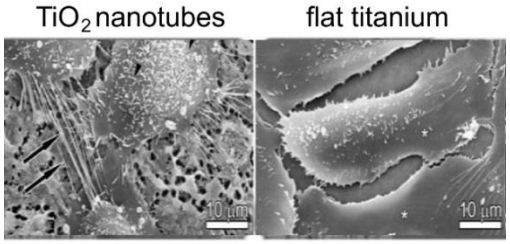

Stimulation of biomaterials growth (stem cells, human osteoblasts, etc.)

Ways of crystallizing TiO_2 NTs

Rapid thermal annealing [*Adv. Mater*., 2008, 20, 4135–4139]
Flame annealing [*J. Phys. D: Appl. Phys*., 2005, 38, 3543–3549]
Water, hydrothermal and hydrothermal vapor treatments at low temperatures [*Nano Lett*., 2011, 11, 3649–3655]
Plasma annealing [*Materials*, 2019, 12, 626]
Microwave annealing [*Mater. Lett*., 2014, 126, 52–54]

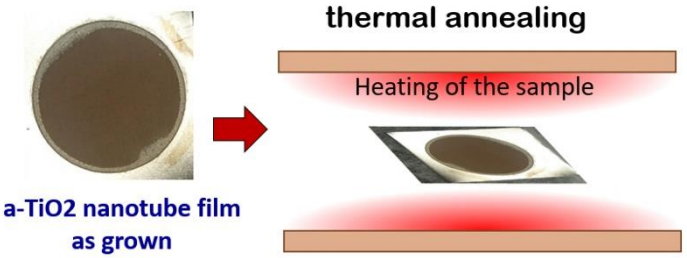

By now none of the listed annealing procedures could replace the thermal annealing in a muffle oven due to, e.g. carbon contamination (flame annealing), very long annealing time in cases of hydrothermal treatments, less developed crystalline phase as compared to oven annealing.

Laser annealing potentially can have several advantages:

- reduced time of annealing
- avoiding oxidation of underlying titanium
- possibility to anneal localized areas, providing annealing patterns

Laser annealing

Previous works

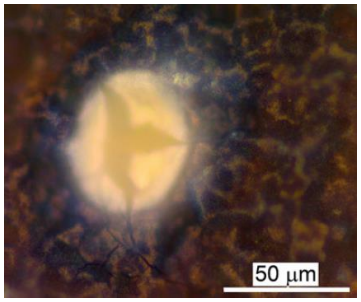

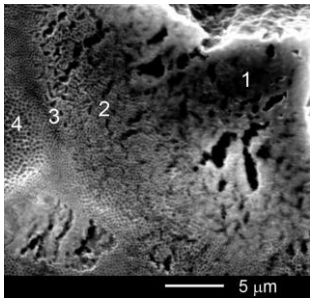

cw, 532 nm laser
Enachi et al. *J. Appl. Phys*. 114, 234302 (2013)
Area 4 corresponds to anatase

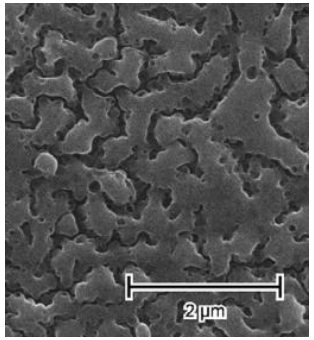

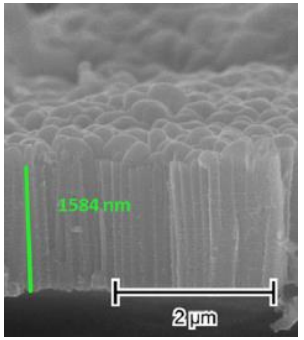

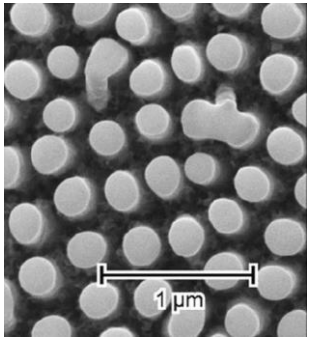

Nd:YAG laser (6 ns, Quantel), 4th harmonics (λ = 266 nm)
Wawrzyniak et al. Appl. Surf. Sci. 508, 145143, (2020); Sci. Rep. 10, 20235 (2020)

The anatase phase was achieved but the tops of TNTs were distorted by melting

In our studies:

IR diode-ns laser	Some sign of anatase [101] phase in XRD spectrum At fluences >150 mJ/cm^2 detachment of NTs from Ti surface
ArF UV ns laser (193 nm)	Mixture of two crystalline phases (anatase + rutile+melting). At fluences > 200 mJ/cm^2, ablation starts
Pharos laser (250 fs, 4th harmonics, 257.5 nm)	No signs of modification after fairly long irradiation. Not enough laser power.
HiLASE ps laser (PERLA-C) 4th harmonics, 257.5 nm, > 50 µJ, 100 kHz	Crystallization to single anatase phase at fluences about 300-400 µJ/cm^2 for ~2 min irradiation at 100 kHz (~several millions of shots). Preserved morphology, crystallite size ~60 nm

The TNT layers were provided by the group of Dr. Jan Macak, Pardubice University

Picosecond UV-laser annealing

Counterintuitive, at first sight, the regime is the most successful

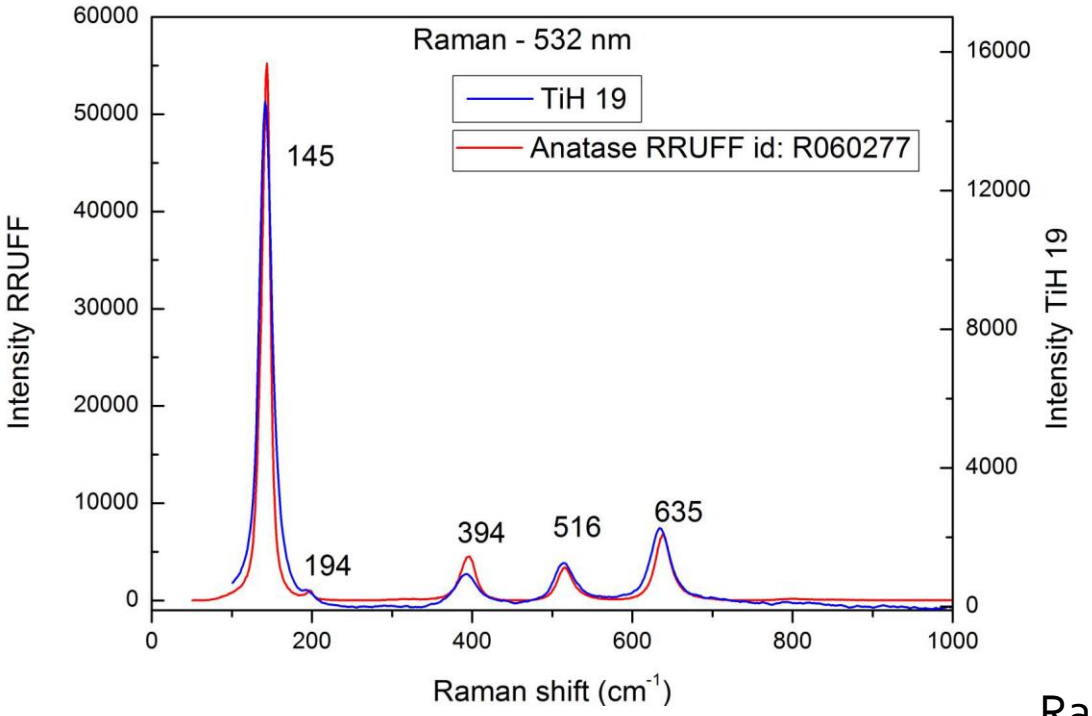

Transformation to violet/black colour is an indication of colour centers and anatase phase

Raman characterization of PERLA-C annealed samples was proved by spectra comparison with internal and online available RRUFF database. Spectrum clearly shows the agreement with crystal phase TiO_2–anatase.

Large area annealing

~ 2 mJ/cm², no focusing

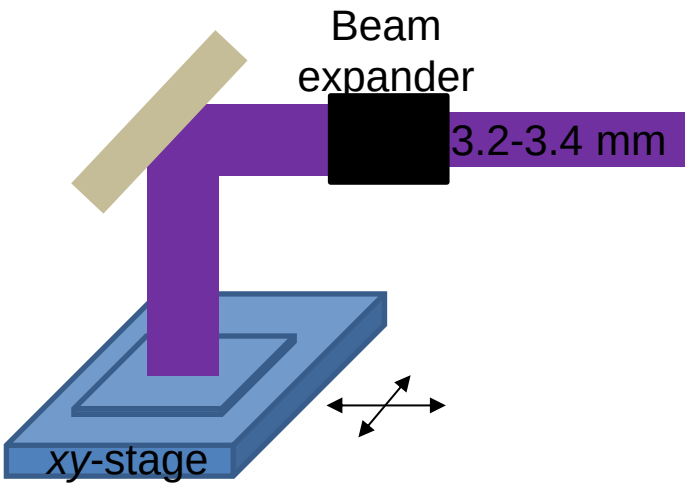

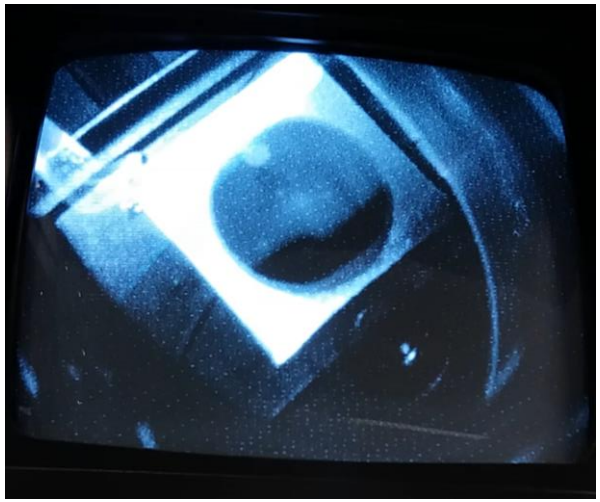

No signs of melting: *explosive solid phase crystallization*

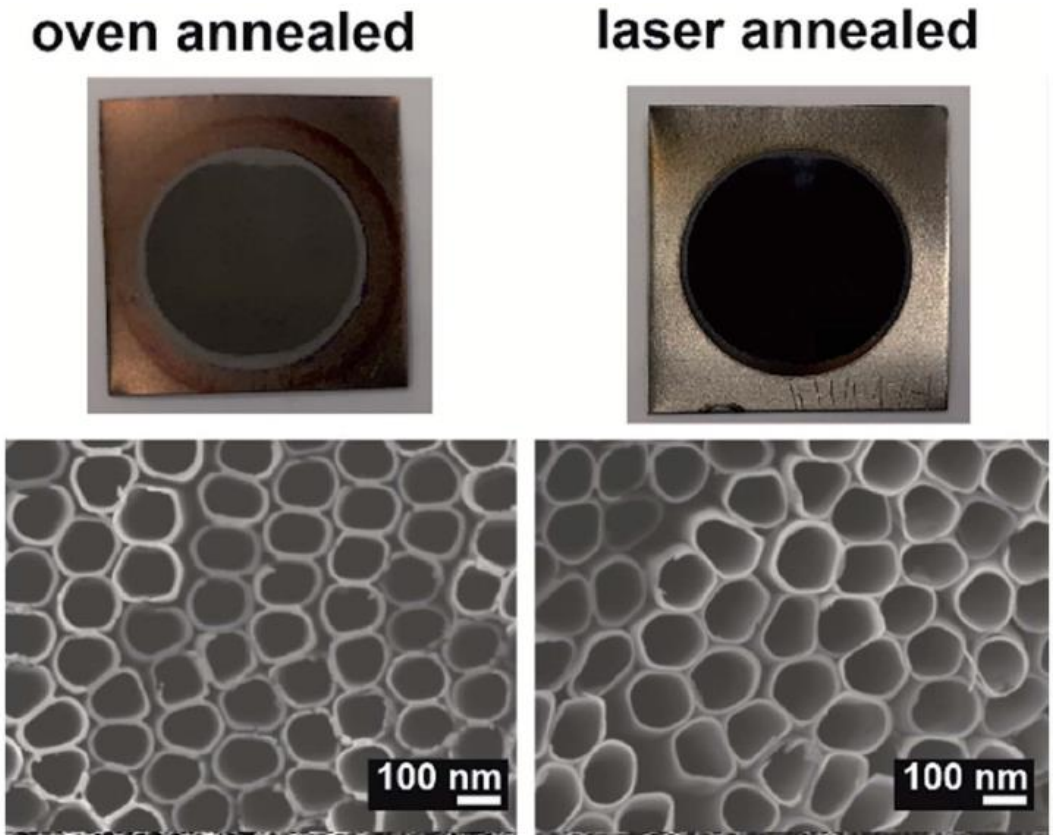

Hanna Sopha et al., *RSC Adv*. 10, 22137–22145 (2020)

Explosive solid-phase crystallization

Mechanism of crystallization:

- Pressure-induced crystallization is a known phenomenon, which is the transition from the low density amorphous to a higher density (pressurized) amorphous phase, followed by pressure induced crystallization (see, e.g., Pandey et al., *J. Appl. Phis.* 109, 113511 (2011))
- Ultrashort laser heating of a surface (absorption) layer may yield a strong shock wave propagating toward the sample depth (Zhigilei et al., *J. Phys. Chem. C* 113, 11892–11906 (2009))
- Shock wave ignites crystallization of metastable amorphous material resulting in a self-propagating wave of crystallization (e.g., Rogachev et al., *Appl. Phys. Lett.* 111, 093105 (2017)) along the nanotubes

Estimation of heating:

Absorbed energy density

$$E_{ab} = (1\text{-}R)\cdot F\ (J/cm^2)/d$$

(in the depth d ~ 100 nm)

Heating: $C\Delta T = E_{ab}$

$\Delta T \approx 125$ K at 2 mJ/cm^2 (peak fluence)

Heat release upon crystallization is of ~22.6 kJ/mol

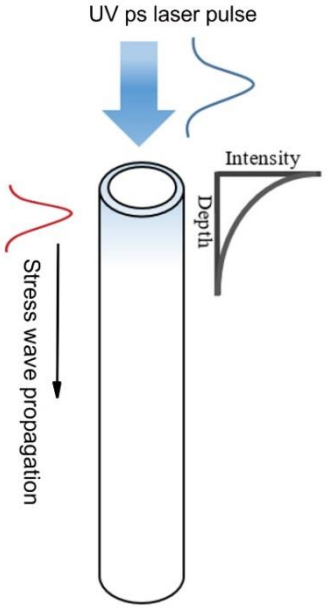

Estimation of stress:

$$\sigma_z = E\alpha\ (T_0 - T_{max})/(1 - \mu)$$

(hollow cylinder, W.D.Kingery, *J. Am. Ceram. Soc*. 38, 3-15 (1955))

This yields ≈ -560 MPa

Compression strength of TiO_2 is 680 MPa

I. Mirza, et al., *Front. Nanotechnol.* **5** (2023) 1271832

Formation of anatase phase

According to Ostwald's rule, transformation proceeds first not to the most stable phase (rutile in the case of TiO2) but to a least stable polymorph closest in energy to the original state (to anatase for TiO2 although it is metastable phase)

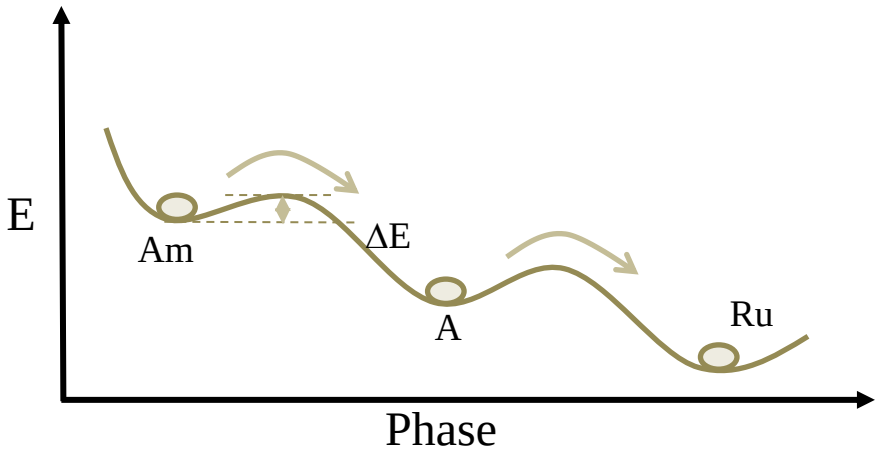

Am: amorphous, Ru: rutile, A: anatase

Activation energies ΔE for amorphous-to-anatase transformation are 69 kJ/mol and anatase-to-rutile transformation are 129 kJ/mol

On the release path of the shock wave, the sequence of observed phase transitions depends on whether the pressure is reduced slowly or rapidly or, by other words, if the new crystalline phase is frozen or can further transform into a more stable phase.

I. Mirza, et al., *Front. Nanotechnol.* **5** (2023) 1271832

Conclusions

- On the examples of two practically important nanoscale amorphous semiconductors, Si-Ge multilayer stacks and titania nanotubes, we have demonstrated that ultrashort laser pulse irradiation can be a good alternative to traditional annealing methods, enabling highly selective localized crystallization.
- Optimal regimes of laser-induced annealing have been revealed when the laser-irradiated samples are converted to crystalline forms without any signs of melting.
- In both cases, we have attributed the melting-free crystallization to the mechanism of stress-induced solid-phase transformation which can be achieved only under the action of ultrashort laser pulses providing conditions of stress confinement.
- The technique of gentle annealing of amorphous materials by ultrashort-pulse laser irradiation is foreseen to be universal for a wide range of nanostructured semiconductors via controllable application of fundamental knowledge of nonequilibrium ultrafast processes.

Acknowledgements

Operational Programme Johannes Amos Comenius and financed by European Structural and Investment Funds and the Czech Ministry of Education, Youth and Sports (project SenDiSo, No. CZ.02.01.01/00/22_008/0004596)

Czech Science Foundation (GACR), project 22-38449L.

SENDISO

Co-funded by the European Union

MINISTRY OF EDUCATION, YOUTH AND SPORTS

GAČR CZECH SCIENCE FOUNDATION

FZÚ

17

Thank you for your attention!

hilase